Transport phenomena in the Co-based zero-gap semimagnetic semiconductor: $Hg_{1-x}Co_xSe$

M. Averous, C. Fau, S. Charar, M. El Kholdi, and V. D. Ribes
Groupe d'Etude des Semiconducteurs, Université Montpellier II, Place E. Bataillon 34095, Montpellier CEDEX 5, France

Z. Golacki
Institute of Physics, Polish Academy of Sciences, Al. Lotnikow 32/46,02-668 Warsaw, Poland
(Received 22 April 1992; revised manuscript received 11 August 1992)

Transport experiments are performed on semiconducting compound $Hg_{1-x}Co_xSe$ with $0<x\leq 0.0087$. Two kinds of phenomena are observed: an enhancement of the mobility $\mu(T)$ when x increases up to 0.0045, followed by a decrease of μ for x between 0.0045 and 0.0087. This behavior, previously seen in $Hg_{1-x}Fe_xSe$, could be explained by the energy position of the uppermost occupied cobalt d level in the conduction band. This leads to a resonance effect and a damping of the conduction electrons via the hybridization of the d level with the s conduction band, and which changes mobility. Near the solubility limit ($x=0.01$), a dip in the mobility curve appears between 10 and 80 K, corresponding to two phase transitions. The dip is probably due to the presence of macroscopic clusters of a cobalt compound, which undergo magnetic phase transitions at these temperatures.

I. INTRODUCTION

Diluted magnetic semiconductors (DMS's) are compound materials in which a fraction of the cations are magnetic. For many purposes one may regard a DMS as being composed of two subsystems. The magnetic subsystem consists of $3d$ magnetic ions and the electronic subsystem consists of the s-like electrons and p-like holes. The most striking phenomena arise from the interactions between these two subsystems.[1-6] The influence of magnetic ions on the transport properties is related to the energy position of the open d-like shell relative to the Fermi level and the band edges. These transport effects, known for a long time, allow for a wide range of possibilities. Using different hosts one observes that the distances between the energy levels of a transition metal remain approximately the same. In $Cd_{1-x}Mn_xSe$ the uppermost occupied one-electron level, with Mn in the 2^+ charge state, occurs in the valence-band continuum. The most studied DMS's contain Mn^{2+} ions, each with a spin $S=\frac{5}{2}$. In many respects Fe-based compounds exhibit entirely different properties than materials containing Mn. This is due to the fact that Fe^{2+} contains one more electron in the $3d$ shell than the half-filled $3d$ shell of Mn^{2+}. If an even number of d electrons are involved, Kramer's theorem cannot be applied and the ground state of the Fe^{2+} ion is a magnetic singlet. In addition, the relatively high energy of the uppermost occupied level of the Fe^{2+} ion is in most cases above the top of the valence band.[4,7,8] Therefore in the case of symmetry-induced zero-gap materials, such as HgSe, the uppermost occupied $3d$ level is degenerate with the conduction band. The case of HgTe is an exception, for which the uppermost $3d$ level is estimated to occur approximately 170 meV below the valence-band edge.[4]

The Co^{2+} free ion has a $3d^7$ electronic configuration, which leads to a $^4F_{9/2}$ ground level. The value $J=\frac{9}{2}$ is determined by the spin-orbit interaction. In a crystal, the magnetic ion is subjected to a crystal field, which is stronger than the spin-orbit interaction. Accordingly, the energy levels in the crystal are obtained by starting from the ^4F level and applying the crystal-field perturbation first, followed by the spin-orbit interaction. The theory indicates that in the zinc-blende structure the ground level is fourfold degenerate and it is well separated from the first excited level (by about 3500 cm^{-1}). The ground level can be described then by an effective spin $S=\frac{3}{2}$. The g factor of this ground level is typically 15% larger than the spin-only value $g=2.0$.[5] However, in transport as well as in photoemission experiments it is very important to know the contribution of the Co $3d^7$ electrons to the Γ_8 band structure. The influence of d electrons on the valence-band density of states (DOS) has been investigated in the case of Mn-based compounds and Fe-based compounds by photoemission, and treated theoretically.[7-9] In the case of Fe the proposed diagram is shown in Fig. 1. The degenerate Fe $3d$ levels are split into a spin-up ($3d^5$) and a spin-down manifold $3d^1$ due to intrashell exchange interaction. In the tetrahedral crystal field the $3d^5\uparrow$ and $3d^1\downarrow$ states are further split into $t_{2g}\uparrow$

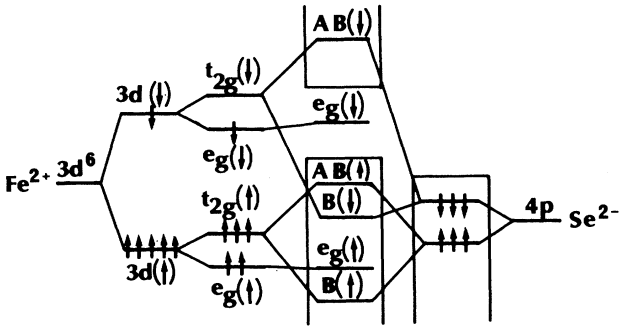

FIG. 1. Schematic energy diagram showing how the Fe-derived DOS is formed from the atomic orbitals in $Cd_{1-x}Fe_xSe$ (from Refs. 7 and 8).

($3d^3$), $e_g\uparrow$ ($3d^2$), $t_{2g}\downarrow$ ($3d^0$), and $e_g\downarrow$ ($3d^1$) states. As a result of different degrees of the wave-function overlap there is no strong Se $4p$–Fe $3d$ (p-d) hybridization for the Fe $e_g\uparrow$ and $e_g\downarrow$ states. The Fe $t_{2g}\uparrow$ and $t_{2g}\downarrow$ states hybridize significantly with the Se $4p$ states ($\uparrow$ and $\downarrow$) and add the Fe $3d$ character to the top 6 eV region of the valence bands. Coupling between the spin-up (spin-down) state produces a bonding $B(\uparrow)$ [$B(\downarrow)$] and an antibonding AB($\uparrow$) [AB($\downarrow$)] level. The schematic diagram in Fig. 1 enables one to interpret all the photoemission spectra of $Cd_{1-x}Fe_xSe$. In the case of $Hg_{1-x}Fe_xSe$ the only difference is the gap (which is zero), which means that the level $e_g\downarrow$ is in the conduction band. This result is in agreement with the transport measurements on $Hg_{1-x}Fe_xSe$.[10] The photoemission spectra obtained on $Cd_{1-x}Fe_xSe$ and $Cd_{1-x}Co_xSe$ are very similar.[11] Although the band structure as well as configuration-interaction calculations are necessary, it is reasonable to assume that the situation in $Hg_{1-x}Co_xSe$ is very similar to that in $Hg_{1-x}Fe_xSe$. The $e_g\downarrow$ level lies in the conduction band. The difference between Fe and Co is the number of electrons: In Fe, $e_g^1\downarrow$ and in Co, $e_g^2\downarrow$.

II. EXPERIMENTAL RESULTS AND INTERPRETATION

The crystals were synthesized by the Bridgman method. The cobalt concentration x was in the range 0–0.0087. The shape of each sample was a parallelepiped with its long dimension in the (110) plane. Figure 2 gives the Hall mobilities of $Hg_{1-x}Co_xSe$ samples as a function of T for four values of x (0.0045, 0.0057, 0.0065, and 0.0087). These values have been deduced from the resistivity and the Hall-effect measurements, assuming one-type carriers. Thus we have $n=1/eR_H$ and $\mu=R_H/\rho$, where R_H is the Hall coefficient and ρ is the resistivity. The four samples have similar carrier concentrations, $(1.2-1.4)\times10^{18}$ cm^{-3} at 4.2 K, and they are almost constant with T. The cobalt concentration x has been deduced from the magnetization curves at 4.2 K. The magnetization data are shown in Fig. 3. They were fitted to the modified Brillouin function,[12]

$$M(B)=\frac{g\mu_B SxN_A}{m(x)}B_S\left[\frac{g\mu_B SB}{k_B T_{\text{eff}}}\right] . \quad (1)$$

Here m is the molar mass,

$$m(x)=(1-x)m_{\text{Hg}}+xm_{\text{Co}}+m_{\text{Se}} , \quad (2)$$

N_A is the Avogadro number, B_S is the Brillouin function, T_{eff} is the effective temperature, μ_B is the Bohr magneton, $S=\frac{3}{2}$ is the effective spin for Co^{2+}, and g is the effective Landé factor. We have determined the effective Landé factor by electron spin resonance (ESR) and found $g=2.3$, in agreement with Ref 13. The effective temperature T_{eff} may be written as

$$T_{\text{eff}}=T+T_0 , \quad (3)$$

where T_0 is a phenomenological parameter, which accounts for the interactions between the magnetic ions. Because of the very low Co^{2+} concentration, $x<1\%$, we consider only the contribution of isolated ions to the magnetization. The cobalt concentration x and the phenomenological temperature T_0 were taken as fitting parameters (Table I). Positive T_0 values (T_{eff} greater than the real temperature) imply an antiferromagnetic interaction at 4.2 K. The magnetization data yield a more precise value of x than microprobe analysis for our very low Co concentrations. The magnetization data were obtained with a superconducting quantum interference de-

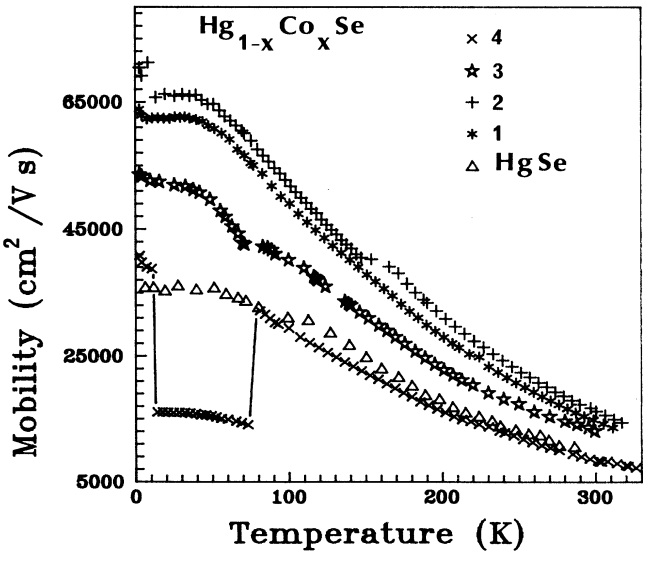

FIG. 2. Hall mobility of $Hg_{1-x}Co_xSe$ and HgSe (Ref. 14) samples as a function of T. For samples 1, 2, 3, and 4 the mole fractions of Co are, respectively, 0.0045, 0.0057, 0.0065, and 0.0087.

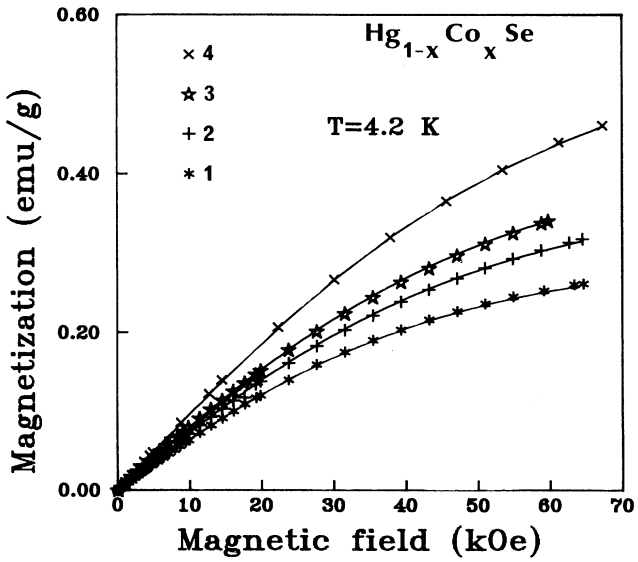

FIG. 3. Magnetization as a function of magnetic field at 4.2 K. Symbols: experimental points. Solid lines: the modified Brillouin's-function fit.

TABLE I. Numerical values of mole fraction x of Co, experimental mobilities μ at 4.2 K, and phenomenological parameter T_0 for $Hg_{1-x}Co_xSe$ samples.

Sample	Symbol	x	μ ($cm^2/V\,s$)	T_0 (K)
1	*	0.0045	6.29×10^4	2
2	+	0.0057	6.91×10^4	2.5
3	☆	0.0065	5.34×10^4	2.8
4	×	0.0087	3.98×10^4	3.8

vice (SQUID) system. The magnetic-moment resolution of this SQUID system changes from 10^{-7} to 10^{-6} emu in the magnetic-field range 5 Oe–70 kOe and the temperature range 1.5–400 K. It is therefore easy to measure magnetic moments of 10^{-4} emu with a sensitivity $\Delta M/M=10^{-3}-10^{-2}$. In Fig. 2 the temperature dependence of the mobility of a HgSe sample (without cobalt) has been added (cf. Ref. 14). This HgSe sample had a carrier concentration close to that of the samples analyzed here. One should notice that the carrier concentrations are almost constant with T. This means that the samples are degenerate and the Fermi level E_F is located in the conduction band. Using the band parameters of HgSe (since x is very small) we calculated E_F. Figure 4 shows the dependence of the Fermi level on carrier concentration in the case of the zero-gap HgSe. The Kane equation[15] has been solved, taking into account the change of the Γ_6-Γ_8 negative optical gap with T.[17] The E_F value calculated for our $Hg_{1-x}Co_xSe$ samples is 110 meV. The mobility curves of the first three samples are higher than that of the HgSe sample in Fig. 2. On the other hand, the fourth sample follows the HgSe curve rather closely, except in the range 10–80 K. In this range the mobility suddenly falls from 3.9×10^4 to 1.6×10^4 $cm^2/V\,s$ at 10 K, and then maintains this low value until 80 K, where it suddenly returns to the HgSe curve. As a result, there are two different behaviors to explain. The first is the enhancement of the mobility with the Co concentration and the second is the dip in the mobility when the first effect has disappeared.

The first effect (mobility enhancement) could be explained in terms of the Mycielski model[18] introduced for the case of $Hg_{1-x}Fe_xSe$, which is very similar to $Hg_{1-x}Co_xSe$. Figure 5 illustrates the electron concentration and mobility versus Fe concentration in $Hg_{1-x}Fe_xSe$, from Ref. 19. The electron concentrations of the $Hg_{1-x}Co_xSe$ samples, (deduced from Hall data) and the Hall mobilities at 4.2 K are plotted versus Co concentration in Fig. 6. In the $10^{-3}-10^{-2}$ mole fraction range of Co the same behavior is observed as in the case of $Hg_{1-x}Fe_xSe$. Following Mycielski, this behavior could be due to the presence of a mixed-valence regime. The $e_g\downarrow$ ($3d^2$) lies in the conduction band and then Co^{2+} acts as a double donor. Our experiments on $Hg_{1-x}Co_xSe$ were carried out in the region where n is rather independent of x. On the other hand, for $Hg_{1-x}Fe_xSe$ (Fig. 5), one can see that n increases with x, for $x<2\times10^{-4}$, reflecting the donor characteristic of Fe. The fact that n is almost constant for x higher than 4.7×10^{-4} indicates a pinning of the Fermi level by the d states and consequently enables one to determine the position of the resonant state with respect to the conduction-band edge that leads, for $e_g\downarrow$ ($3d^2$) Co level, to 110 meV above the bottom of the conduction band. In the mixed-valence region a strong suppression of the mobility is expected. This suppression is not only due to the scattering by ionized Co atoms, but also to an efficient scattering when E_F coincides with the Co level. Except for sample 4, where a drop of μ could be seen between 10 and 80 K, the mobility data of samples 1–3 do not follow this prediction. The

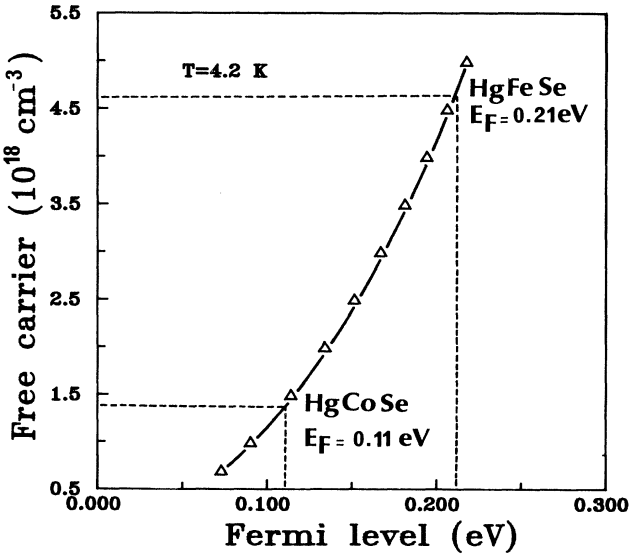

FIG. 4. Calculated Fermi-level position vs carrier concentration at 4.2 K, obtained from an exact solution at the Kane equation. E_F of $Hg_{1-x}Fe_xSe$ correspond to Ref. 16.

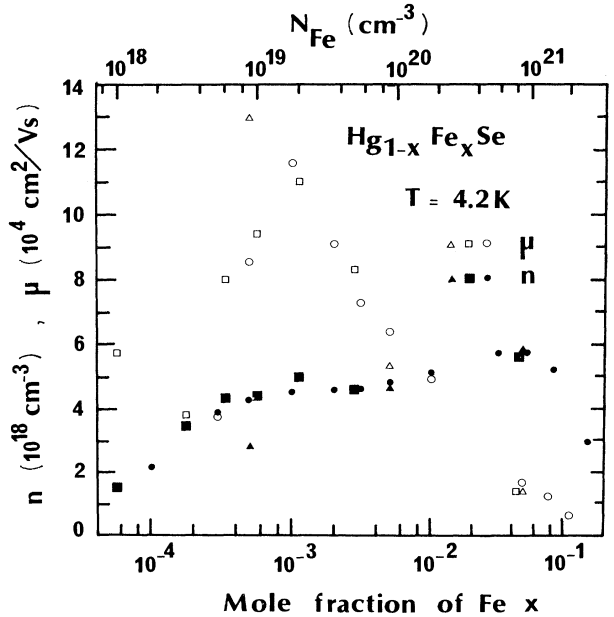

FIG. 5. Electron concentration n and Hall mobility μ vs Fe concentration in $Hg_{1-x}Fe_xSe$ at 4.2 K. The data are taken from Ref. 3 (○,●); Ref. 20 (△,▲); and Ref. 21 (□,■).

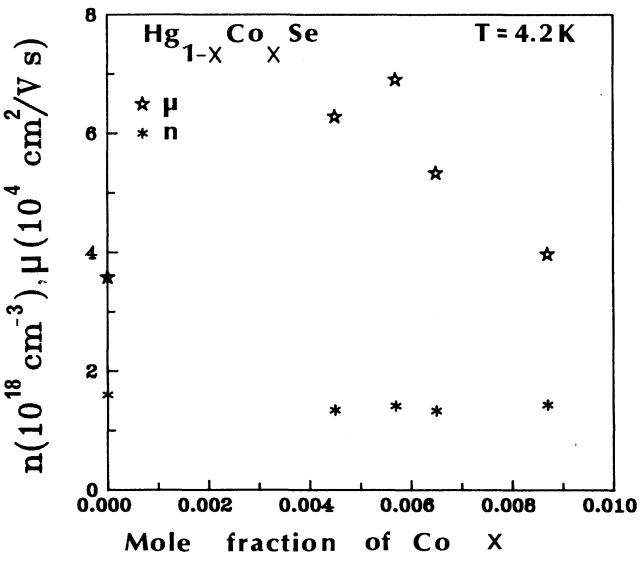

FIG. 6. Electron concentration n and Hall mobility μ vs Co concentration in $Hg_{1-x}Co_xSe$. Our results are used for $Hg_{1-x}Co_xSe$; those of Ref. 14 are used for HgSe.

mobility curves indicate that μ increases with respect to that in HgSe by a factor of 4.4 at about the same carrier concentration. This high mobility shows that the scattering rate of conduction electrons at low temperatures is greatly suppressed in the mixed-valence region.

Mycielski[18] interpreted the observed reduction in scattering. He proposed that a "superlattice" of ionized donors is formed as a result of the Coulomb repulsion between their charges. In such a system of ordered charges there is less scattering of the conduction electrons than by randomly distributed ionized donors. Another consequence of the Coulomb interdonor interaction is the appearance of the Coulomb gap in the one-electron density of impurity states.[18,22,23] The existence of the Coulomb gap is thought to be responsible for the absence of resonant scattering. In spite of its interesting features this model is not without drawbacks. If one looks carefully at the experimental data, it appears that the temperatures at which the high-mobility anomalies disappear ($T > 100$ K for $Hg_{1-x}Fe_xSe$ or $T > 200$ K for $Hg_{1-x}Co_xSe$) are too high for the ion magnetic ordering temperature. A crude estimate of the mean distance between charged donors is comparable to the screening radius. This screening reduces the Coulomb interaction between ionized magnetic ions. Tsidil'kovskii[24] has shown that it is difficult to expect that a strictly regular lattice will be formed. Finally, it is difficult to imagine Wigner-type crystallization in the region where all Co ions are ionized, because of the random distribution of magnetic ions (see Fig. 6).

Kuleev *et al.*[25] have proposed an alternative explanation of the mobility enhancement in $Hg_{1-x}Fe_xSe$, related to the hybridization of s and d electrons and background scattering. The authors consider the Anderson Hamiltonian[26] for a systems of electrons interacting with chaotically distributed d impurities and a random scattering field. The d states of the iron impurity can be occupied by one (Fe^{3+}) or two (Fe^{2+}) d electrons, and the transition $d^1 \rightleftarrows d^2$ determines the energy of the d resonance. In order to calculate both the renormalized energy spectrum and the damping one has to go to the third-order terms in the s-d hybridization constant. It has been found that the introduction of d impurities results in a radical reconstruction of the electronic spectrum: these appear as two branches characterized by their own dampings. The spectrum changes are substantial in the vicinity of the resonance level. As for the damping, there is no resonance peak in the neighborhood of the d level. Far from the resonance, the electronic states possess an s-like character and their damping is $\Gamma_{1,2}(\varepsilon_k) \sim \gamma_\phi$ for both branches. However, in the vicinity of the resonance, $E \approx \Omega$, the electronic states posses a d-like character because of the s-d hybridization and their damping diminishes to the width of the d level: γ_d. In order to calculate the electronic relaxation time $\tau(E)$, the relation $\hbar/\tau(E) = \Gamma(E)$ has been used, in which $\Gamma(E)$ is the imaginary part of the self energy. It has been shown that, if $\gamma_d < \gamma_\phi$, the collision-broadening $\Gamma(E)$ has a minimum at the resonance, which corresponds to the maximum of the relaxation time, i.e., to a maximum of mobility. As a consequence, Kuleev *et al.* have shown that, both as a function of the iron density N_d and the temperature, the mobility can have a maximum as a result of interplay between the background scattering and the resonant scattering. Figure 7 shows their results for the dependence of conduction electron mobility on temperature for various N_d. From curves 1–3, it follows qualitatively that when N_d increases the whole curve of $\mu(T)$ shifts toward higher values. However, a further increase of N_d (curve 4) shifts mobility toward lower values. The samples used in our work displayed the same general behavior, with the highest μ corresponding to $x_{Co} = 0.0057$ (cf. Fig. 2).

The second effect, i.e., the drop of mobility for sample 4, occurs for $x = 0.0087$ at $T = 10$ K. The mobility re-

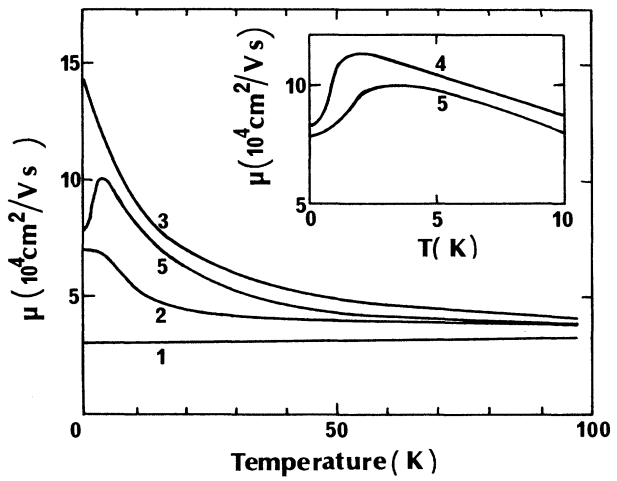

FIG. 7. Theoretical temperature dependence of conduction-electron mobilities. (1) $N_d = 4\times10^{18}$ cm^{-3}; (2) 5×10^{18} cm^{-3}; (3) 8×10^{18} cm^{-3}; (4) 2×10^{19} cm^{-3}; (5) 5×10^{19} cm^{-3}. Data from Ref. 25.

turns to the value for HgSe at about 80 K. Outside the range 10 K $< T <$ 80 K, the $\mu(T)$ curve follows rather well the curve for HgSe with the same carrier concentration. The behavior of $\mu(T)$ for HgSe is understood in terms of scattering by charged centers and by optical phonons. The acoustic phonons do not play an important role at temperatures below 300 K (see, for example, Ref. 14). This drop of $\mu(T)$ between 10 and 80 K for the highest Co concentration seems strange. The first idea is to attribute the drop of μ to a classical resonant level with an efficient resonant scattering mechanism. It is well known that such a resonance decreases the mobility, but it has never been observed to lead to an *abrupt* change of μ. To resolve this puzzle additional experiments were performed. The same experiments were performed several months later. The amplitude of the dip in μ was found to be smaller. Moreover, the anomaly in μ disappeared when the magnetic field increased from zero to $B=1$ T. Using these results one can imagine that the dip in μ is caused by metastable macroscopic inclusions containing large concentration of Co ions. These inclusions appear when the Co concentration increases until it is near the solubility limit. Investigating $Hg_{1-x}Eu_xSe$ with $x=10^{-3}$, Krylov *et al.*[27] observed a sharp increase of $\rho(T)$ at $T=4.5$ K. Their carrier concentration was constant with T. They suggest the existence of EuSe clusters. Although not indicated by the authors, that explanation is strongly supported by the magnetic phase diagram of EuSe,[28] where the temperature of the anomaly on ρ is exactly the same as that of the magnetic phase transition of EuSe.

In order to support the assumption of clusters in our samples of $Hg_{1-x}Co_xSe$ with large Co concentration, we have performed a Co profile by energy dispersion spectrometry (EDS). It is confirmed that there exist randomly distributed regions where the Co concentration is high with respect to the background. Alloys of Co with Se could be CoSe, Co_2Se_3, or Co_8Se_9. Unfortunately, the magnetic phase diagram of such alloys were unknown until the present. One can imagine the following sequence of transitions for the clusters as T increases: antiferromagnetic or spin glass to ferromagnetic near 10 K, and then ferromagnetic to paramagnetic at 80 K. The magnetic moments in the clusters are then zero below 10 K, finite between 10 and 80 K, and zero above 80 K. In the antiferromagnetic or spin-glass phase the magnetic moments of randomly distributed clusters are zero and thus have no influence on the spin scattering. In the ferromagnetic phase the charge carriers are scattered by the magnetic moments of the randomly distributed clusters. Once they reach the paramagnetic region the additional scattering processes due to the magnetic moment of the clusters disappear and the mobility has a normal behavior. Obviously, this phenomenon becomes large when x approaches the limit of solubility, about 1%. However, as a result, when one looks carefully at the other curves (Fig. 2) the pit effect can be observed, but in a smaller capacity.

The existence of the clusters also affects the magnetization. In order to support the assumption of a ferromagnetic phase of Co selenide clusters between 10 and 80 K,

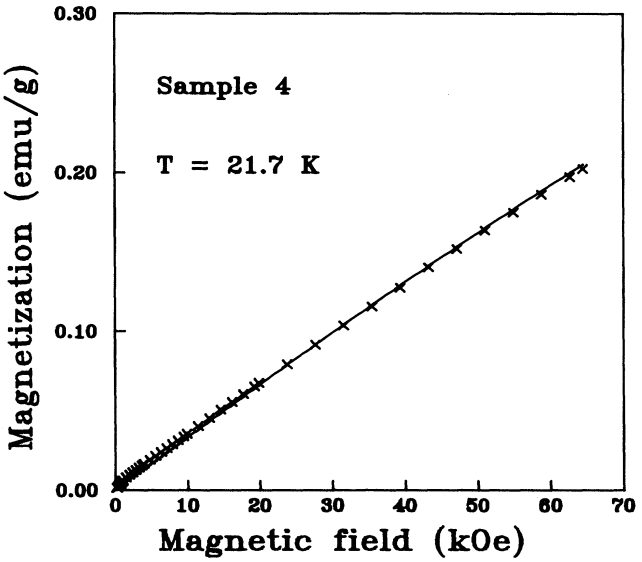

FIG. 8. Magnetization as a function of B for sample 4 at 21.7 K up to 70 kOe ($x=0.0087$, $T_0=1.5$ K).

used to explain the pit mobility, we have performed[29] for sample 4 magnetization at 21.7 K (inside the temperature range of the pit); see Fig. 8. $M(B)$ follows roughly a linear dependence except at low fields. The linear dependence at higher fields is well fitted with the x value determined at 4.2 K and T_0 characteristic of an antiferromagnetic interaction. The low-field part is given in Fig. 9 on an enlarged scale. It can be seen very clearly that $M(B)$ is the sum of two contributions (curves 1 and 2). Curve 1

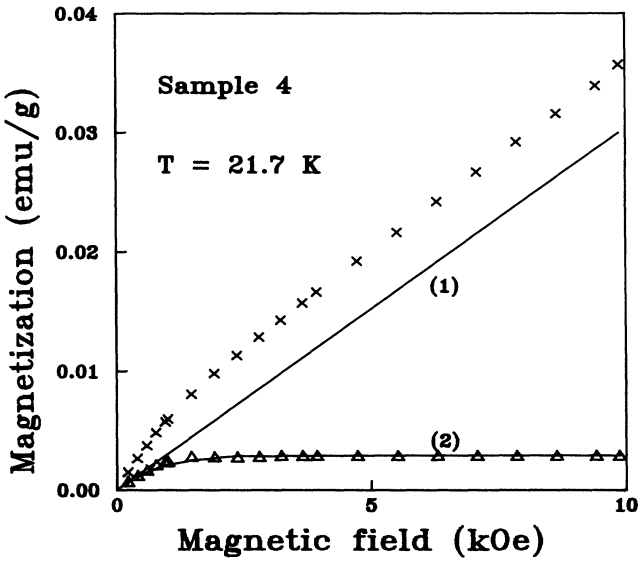

FIG. 9. Magnetization as a function of B in low-field region for sample 4 at 21.7 K. ×, experimental points. Curve 1: High-field curve extrapolated, fitted with isolated Co^{2+}. Curve 2 represents the clusters contribution. Symbols (Δ) are values obtained by subtracting curve 1 from the experimental values. The solid line is the fit of Δ points with $S_0=\frac{3}{2}$, $x=4.2\times10^{-5}$, and $T_0=-21.6$ K.

corresponds to the antiferromagnetic contribution deduced at high field. Curve 2 is characteristic of ferromagnetic interactions. Because the saturation is very quickly reached we can deduce easily from the saturation limit the values of x and T_0 which enable one to fit curve 2: $x = 4.2 \times 10^{-5}$ and $T_0 = -21.6$ K. x represents the concentration of Co^{2+} included in the clusters and T_0 shows clearly the existence of the ferromagnetic phase of the cluster.

III. CONCLUDING REMARKS

We have observed an enhancement of the $\mu(T)$ curves when Co ions are introduced in HgSe crystals for Co concentration $x \leq 0.0057$. For x between 0.0057 and 0.0087, $\mu(T)$ decreases and reaches the HgSe mobility value with the same carrier concentration for $x = 0.0087$. This phenomenon could be explained by the energy position of the uppermost occupied level of Co, degenerate in the conduction band. Such a situation could be explained by the effect of d resonance on the spectrum and the conduction-electron damping.

In addition, at $x = 0.0087$ a dip in $\mu(T)$ appears between 10 and 80 K, attributed to the existence of cobalt selenide clusters. This mobility reduction is correlated to the magnetic phase diagram of the randomly distributed cobalt selenide clusters.

ACKNOWLEDGMENTS

The authors wish to thank J. Deportes for his help in magnetization measurements and Dr. Y. Shapira for helpful discussions. This work was supported in part by the Centre National de la Recherche Scientifique and in part by Polish State Committee for Scientific Research Grant No. 22 3149102. The Groupe d'Etude des Semiconducteurs is URA 357.

[1] A. Mycielski, in *Diluted Magnetic (Semimagnetic) Semiconductors,* edited by R. L. Aggarwal, J. K. Furdyna, and S. von Molnar, MRS Symposia Proceedings No. 89 (Materials Research Society, Pittsburgh, 1987), p. 159.

[2] F. Pool, J. Kossut, U. Debska, R. Reifenberger, and J. K. Furdyna, in *Diluted Magnetic (Semimagnetic) Semiconductors,* edited by R. L. Aggarwal, J. K. Furdyna, and S. von Molnar, MRS Symposia Proceedings No. 89 (Materials Research Society, Pittsburgh, 1987), p. 169.

[3] F. S. Pool, J. Kossut, U. Debska, and R. Reifenberger, Phys. Rev. B **35**, 3900 (1987).

[4] A. Mycielski, J. Appl. Phys. **63**, 3279 (1988).

[5] Y. Shapira, in *Semimagnetic Semiconductors and Diluted Magnetic Semiconductors,* edited by M. Averous and M. Balkanski, Physical Sciences No. 55 (Plenum, New York, 1991), p. 121.

[6] M. Averous, in *Semimagnetic Semiconductors and Diluted Magnetic Semiconductors,* edited by M. Averous and M. Balkanski, Physical Sciences No. 55 (Plenum, New York, 1991), p. 1.

[7] M. Taniguchi, Y. Ueda, I. Morisada, Y. Murashita, T. Ohta, I. Souma, and Y. Oka, Phys. Rev. B **41**, 3069 (1990).

[8] C. Benoit à la Guillaume, in *Semimagnetic Semiconductors and Diluted Magnetic Semiconductors,* edited by M. Averous and M. Balkanski, Physical Sciences No. 55 (Plenum, New York, 1991), p. 191.

[9] S. H. Wei and A. Zunger, Phys. Rev. B **15**, 8958 (1988).

[10] T. Dietl, in *Semimagnetic Semiconductors and Diluted Magnetic Semiconductors,* edited by M. Averous and M. Balkanski, Physical Sciences No. 55 (Plenum, New York, 1991), p. 83.

[11] K. Kopalko, B. J. Kowalski, B. A. Orlowski, A. Mycielski, and V. Chab, Acta Phys. Pol. A **77**, 403 (1990).

[12] J. A. Gaj, R. Planel, and G. Fishman, Solid State Commun. **29**, 435 (1979).

[13] T. Hoshina, J. Phys. Soc. Jpn. **21**, 1608 (1966).

[14] T. Dietl and W. Szymanska, J. Phys. Chem. Solids **39**, 1041 (1978).

[15] E. O. Kane, J. Phys. Chem. Solids **1**, 249 (1957).

[16] J. Kossut, W. Dobrowolski, Z. Wilamowski, T. Dietl, and K. Swiatek, Semicond. Sci. Technol. **5S**, 260 (1990).

[17] M. Dobrowolska, W. Dobrowolski, and A. Mycielski, Solid State Commun. **34**, 441 (1980).

[18] J. Mycielski, Solid State Commun. **60**, 165 (1986).

[19] T. Dietl, Proceedings of the 18th International Conference on Low Temperature Physics, Kyoto, 1987 [Jpn. J. Appl. Phys. **26**, 1907 (1987)].

[20] N. G. Gluzman, N. D. Sabirzyanova, I. M. Tsidil'kovskii, L. D. Paranchich, and S. Y. Paranchich, Fiz. Tekh. Poluprovodn. **20**, 94 (1986) [Sov. Phys. Semicond. **20**, 55 (1986)].

[21] W. Dobrowolski, K. Dybko, A. Mycielski, J. Mycielski, J. Wrobel, S. Piechota, M. Placzewska, H. Szymczak, and Z. Wilamowski, in *18th International Conference on Physics of Semiconductors,* edited by O. Engström (World Scientific, Singapore, 1987), p. 1743.

[22] F. H. Pollak, Phys. Rev. A **138**, 619 (1965).

[23] *Electronic Properties of Doped Semiconductors,* edited by B. I. Shklovskii and A. L. Efros, Springer Series in Solid-State Sciences Vol. 45 (Springer-Verlag, Berlin, 1984).

[24] I. M. Tsidil'kovskii (unpublished).

[25] I. I. Kuleev, I. I. Lyapilin, and V. V. Karyagin, Phys. Status Solidi B **163**, 449 (1991), and references therein.

[26] P. W. Anderson, Phys. Rev. **124**, 41 (1961).

[27] K. R. Krylov, A. I. Ponomarev, I. M. Tsidil'kovskii, N. P. Gavaleshko, and V. V. Khomyak, Fiz. Tekh. Poluprovodn. **23**, 3 (1989) [Sov. Phys. Semicond. **23**, 1 (1989)].

[28] R. Griessen, M. Landolt, and H. R. Ott, Solid State Commun. **9**, 2219 (1971).

[29] M. Averous, C. Fau, S. Charar, M. El Kholdi, V. D. Ribes, J. Deportes, and Z. Golacki, Solid State Commun. **84**, 479 (1992).